On Backward Compatibility in GNSS Signal Design

Felix Antreich[(1)], Jean-Jacques Floch[(2)], Jean-Luc Issler [(3)], and Josef A. Nossek [(4)]
(1) *German Aerospace Center (DLR), Germany*
(2) *EADS-Astrium GmbH, Germany*
(3) *Centre National d'Etudes Spatiales (CNES), France*
(4) *Munich University of Technology (TUM), Germany*

BIOGRAPHY

Felix Antreich (IEEE M'06) received the diploma and the Ph.D. in electrical engineering from the Munich University of Technology (TUM), Munich, Germany, in 2003 and 2011, respectively. Since July 2003, he has been with the Institute of Communications and Navigation of the German Aerospace Center (DLR), Wessling-Oberpfaffenhofen, Germany.

Jean-Jacques Floch obtained his engineering diploma in electronics and telecommunication at the Institut Superieur Electronique Numerique, in France in 1998. He has been working in the area of mobile communications for several years. Since 2002 he has been working in the field of navigation satellite as system engineer at the EADS-Astrium GmbH. His work mainly focuses on Galileo signal design at system level and evaluation of performances and robustness of Galileo signals.

Jean-Luc Issler is head of the Instrumentation Telemetry and Propagation Department of the CNES Radio Frequency sub-directorate since August 2009. He works at CNES on GNSS signals, receivers and transmitters since 20 years, and was head of CNES Radio Navigation then Transmission Techniques and Signal Processing Department since 1996. He is delegate to the Galileo Signal Task Force. He received the Astronautic Prize of AAAF (aeronautical and space association) in 2004, and the EADS Science and Engineering prize delivered in 2008 by French Academy of Sciences, for his work on GNSS frequencies and modulations, and, spaceborne RF equipments.

Josef A. Nossek (IEEE S'72–M'74–SM'81–F'93) received the Dipl.-Ing. and the Dr. techn. degrees in electrical engineering from the University of Technology in Vienna, Austria in 1974 and 1980, respectively. In 1974 he joined Siemens AG in Munich, Germany as a member of technical staff, in 1978 he became supervisor, and from 1980 on he was Head of Department. In 1987 he was promoted to be Head of all radio systems design. Since 1989 he has been Full Professor for circuit theory and signal processing at the Munich University of Technology where he teaches undergraduate and graduate courses on circuit and systems theory and signal processing and leads research on signal processing algorithms for communications, theory of linear systems and VLSI architectures.

ABSTRACT

This work further develops tools and methodologies for systematic GNSS signal design. Inter and intra system multiple access interference (MAI), synchronization accuracy, time-delay estimation robustness, and backward compatibility with respect to already existing signals are considered by solving a nonlinear multi-objective optimization problem. Final solutions are selected out of the derived Pareto optimal set and their performance in terms of Cramer Rao lower bound (CRLB) for time-delay estimation considering inter and intra MAI is assessed. Furthermore, implementation aspects with respect to signal generation on the payload and with respect to processing in the receiver including multipath behavior are analyzed.

INTRODUCTION

Chip pulse shape design for timing synchronization with DS-CDMA systems and in particular for Global Navigation Satellite Systems (GNSS) shall provide minimum error in time-delay estimation while also achieving robustness in its estimation. Maximizing the synchronization accuracy can be attained by minimizing the Cramer-Rao lower bound (CRLB) for time-delay estimation. Robustness in the estimation of the time-delay, thus tracking and acquisition robustness can be achieved by limiting the absolute

value of the sidelobes of the autocorrelation function of the signal. Furthermore, bandwidth efficiency is an important objective, as well as maximizing time concentration of the chip pulse shape and providing a fast decay in time domain. Multiple access interference (MAI) and interchip interference (ICI) need to be controlled to maintain system performance [1, 2] and especially for GNSS, we need to account for spectral separation to other signals. Thus, not only intra system MAI but also inter system MAI between different GNSS which transmit signals in the same frequency band has to be considered [3]. Finally, also backward compatibility of a new signal design with respect to already defined or used GNSS signals is of great importance when discussing modernization or evolution of GNSS.

In this work a systematic approach to design optimum strictly band-limited chip pulse shapes for DS-CDMA systems for timing synchronization is further developed based on the work in [4]. The proposed methodology makes it possible to formulate the problem of designing optimum chip pulse shapes in terms of achieving a trade-off between timing synchronization accuracy, time concentration, and backward compatibility of the chip pulse shape while accounting for acquisition and tracking robustness, as a tractable nonlinear multi-objective optimization problem. Additional constraints can be introduced to the problem in order to take into account further properties. Especially, inter system MAI and a fast decay of the chip pulse in time domain (smooth cut-off) is considered. This methodology is based on the prolate spheroidal wave functions (PSWF) [5], which enable to transform the primal variational problem into a dual, tractable parametric optimization problem.

The overall goal of this work together with previous work [4, 6] is to prepare signal optimization tools which will be ready for use when all the signal specifications and constraints for next generation of GNSS will be defined.

SYSTEM MODEL

We assume coherent downconversion of the radio frequency signal to baseband. The received DS-CDMA baseband signal is given by

$$y(t) = \sqrt{P}\, c(t-\tau) + n(t), \tag{1}$$

where P denotes the signal power, $c(t)$ is the pseudo random (PR) sequence, τ is the time-delay, and $n(t)$ is white Gaussian noise with two-sided power spectral density $N_0/2$. Thus, the PR sequence is given by

$$\begin{aligned} c(t) &= \sum_{k=-\infty}^{\infty} d_k \sqrt{T_c}\, \delta(t - kT_c) * h(t) \\ &= \sum_{k=-\infty}^{\infty} d_k \sqrt{T_c}\, h(t - kT_c), \end{aligned} \tag{2}$$

where $h(t)$ denotes the chip pulse shape which is not necessarily restricted to be time-limited to only one chip interval T_c. The PR sequence is a binary, zero-mean wide-sense cyclostationary (WSCS) sequence with $\{d_k\} \in \{-1, 1\}$ and has period $T = N_d T_c$. $N_d \in \mathbb{N}$ denotes the number chips of the PR sequence $c(t)$. The autocorrelation of $c(t)$ can be given by

$$\begin{aligned} R_c(\varepsilon) &= \frac{1}{T} \int_{-\frac{T}{2}}^{\frac{T}{2}} c(t)\; c^*(t+\varepsilon)\; dt \\ &= \int_{-\infty}^{\infty} |H(f)|^2 \mathrm{e}^{\mathrm{j}2\pi f \varepsilon}\; df, \end{aligned} \tag{3}$$

where $H(f)$ denotes the Fourier transform of the chip pulse shape $h(t)$ and the PR sequence is assumed to be random.

STATEMENT OF THE PROBLEM

The objective of this work is to further develop a design methodology based on the work given in [4] to systematically derive optimized chip pulse shapes for DS-CDMA systems for timing synchronization, which are strictly band-limited, thus $H(f) = 0\ ,\ |f| > B$. The optimization is performed with respect to maximizing timing synchronization accuracy, maximizing time concentration of the chip pulse shape within a desired interval of chip duration $[-T_c/2, T_c/2]$, and maximizing backward compatibility to current GNSS signals. Additional constraints can be considered. Maximization of timing synchronization accuracy can be accomplished by minimizing the CRLB for the time-delay τ. Maximizing the time concentration of the chip pulse shape is directly related with the absolute value of the sidelobes of the chip pulse shape and its autocorrelation function $R_c(\varepsilon)$. The maximum of the absolute value of the sidelobes of $R_c(\varepsilon)$ is given by

$$\underset{i \in \mathbb{N}}{\forall} |\nu_i| \leq \kappa, \tag{4}$$

where ν_i denote the value of $R_c(\varepsilon)$ at the sidelobes, besides the global maximum of $R_c(\varepsilon)$ at $\varepsilon = 0$, and $\kappa \in [0, 1]$. The higher κ, the less robust time-delay estimation, and thus tracking and acquisition becomes. Maximizing backward compatibility can be achieved by maximizing the cross-correlation between a current GNSS signal and the new signal design.

Furthermore, for a given spreading gain of the DS-CDMA system, a small time-bandwidth product ϱ is desired in order to ensure bandwidth efficiency. Additionally, intra system MAI, inter system MAI, and ICI are to be considered for the signal design.

Minimizing the CRLB of the time-delay, maximizing time concentration, and maximizing backward compatibility are conflicting tasks and thus only a trade-off between these three objectives can be achieved for a fixed time-bandwidth product ϱ. Such problems are called multiple-objective problems [7], where it is only possible to improve one objective at the cost of the others.

Synchronization Accuracy

The variance of the time-delay estimation error σ_τ^2 of any unbiased estimator is lower bounded by the CRLB [8]

$$\sigma_\tau^2 \geq \frac{B_n}{\frac{P}{N_0}\,4\pi^2}\,\frac{\int_{-\infty}^{\infty}|H(f)|^2\,df}{\int_{-\infty}^{\infty}f^2\,|H(f)|^2\,df}, \tag{5}$$

where B_n denotes the equivalent noise bandwidth of the generic estimator.
The first objective of our trade-off is to minimize σ_τ^2. This minimization is subject to the constraint

$$\int_{-B}^{B}|H(f)|^2\,df = 1. \tag{6}$$

Instead of minimizing (5) considering (6) we can maximize the second moment of the power spectrum $\int_{-\infty}^{\infty}f^2\ |H(f)|^2df$, where it is straight forward to show that

$$\int_{-B}^{B}f^2\,|H(f)|^2\,df \leq \int_{-B}^{B}B^2\,|H(f)|^2df \leq B^2, \tag{7}$$

subject to (6). Thus, $|H(f)|^2 = \frac{1}{2}\left(\delta(f-B)+\delta(f+B)\right)$ maximizes $\int_{-\infty}^{\infty}f^2\,|H(f)|^2df$ and the pulse shape $h(t)$ results to either $h(t) = \cos(2\pi Bt)$ or $h(t) = \sin(2\pi Bt)$. This denotes the analytical solution of the first objective of the trade-off where maximum synchronization accuracy in terms of minimizing the CRLB is achieved.

Time Concentration

The second objective of our trade-off is to maximize the time concentration of $h(t)$ within the interval $[-T_c/2, T_c/2]$. This also achieves better acquisition and tracking robustness by minimizing the sidelobes of $h(t)$ and consequently the sidelobes of $R_c(\varepsilon)$ (low κ).
It has been shown in [5] that for any time-bandwidth product $\varrho = T_cB$

$$\int_{-T_c/2}^{T_c/2}|h(t)|^2dt \leq \chi_0(\varrho), \tag{8}$$

subject to (6). Here, $\chi_0(\varrho)$ is the eigenvalue of the function $\psi_0(\varrho,t)$. The function $\psi_0(\varrho,t)$ has the largest eigenvalue of the PSWF [5]. Hence, the extremal solution of the second objective of our trade-off can be given in closed form solution by $h(t) = \psi_0(\varrho,t)$.

Backward Compatibility

The third objective of our trade-off is to maximize backward compatibility with respect to a current GNSS signal design. Following (3) backward compatibility can be quantified by the cross-correlation between the chip pulse shape of a new signal design $h(t)$ and the chip pulse shape $h_b(t)$ of a current GNSS signal given that the binary PR sequence and the the chip duration T_c are equivalent for both. Hence, we define

$$b = \left[\int_{-B}^{B}H_b^*(f)\,H(f)\,df\right]^2, \tag{9}$$

where $H_b(f)$ denotes the Fourier transform of $h_b(t)$. Assuming that $\int_{-B}^{B}|H(f)|^2\,df = 1$ and $\int_{-B}^{B}|H_b(f)|^2\,df = 1$ and applying the Schwarz inequality it can be shown that

$$0 \leq b \leq 1. \tag{10}$$

Obviously, the extremal solution of the third objective of our trade-off can be given in closed form solution by $h(t) = h_b(t)$.

Smooth Cut-Off

Considering a real physical system a smooth cut-off of $H(f)$ at $\pm B$ is desirable, where $H(f)$ is strictly band-limited to $[-B,B]$ and $H(f)$ is assumed to be continuous in $[-B,B]$. Thus, we define the constraint

$$H(f) = 0\ ,\ |f| = B. \tag{11}$$

A smooth cut-off provides a faster asymptotic decay of $h(t)$ for $t \mapsto \pm\infty$ and thus this leads to less time support which is needed in signal generation.

Interchip Interference (ICI), Intra and Inter System Multiple Access Interference (MAI)

Following, [9, p.23 et seq.], and [1, 2, 3] we consider ICI, intra system MAI (MAI-A) and inter system MAI (MAI-R) as interference components with zero mean. In general ICI and both MAI-A and MAI-R are dependent on the propagation characteristics of the transmitted signal. We consider U users (e.g. visible GNSS satellites) with $u = 1,\ldots,U$ and power P_u causing MAI-A. Further, we assume that V users of another system (e.g. visible satellites of a different GNSS) with $v = 1,\ldots,V$ and power P_v are causing MAI-R. The received signal of another system in the same frequency band has power spectrum density (PSD) $\Phi_R(f)$. Thus, the ratio of the signal to noise ratio (SNR) with respect to the signal to interference plus noise ratio (SINR)

can be given as [9, p.23 et seq.]

$$\Delta\text{SNR} = \frac{\text{SNR}}{\text{SINR}} = 1 + \underbrace{\frac{P\,2T_c}{N_0} \sum_{\substack{l=-\infty \\ l\neq 0}}^{\infty} \left[\int_{-\infty}^{\infty} |H(f)|^2 \cos(2\pi l T_c f)\, df\right]^2}_{\text{ICI}} + \underbrace{\sum_{u=1}^{U} \frac{P_u}{N_0} \int_{-B}^{B} |H(f)|^4\, df}_{\text{MAI-A}} + \underbrace{\sum_{v=1}^{V} \frac{P_v}{N_0} \int_{-B}^{B} |H(f)|^2\, \Phi_R(f)\, df}_{\text{MAI-R}}. \quad (12)$$

In our problem at hand we will take into account ICI and MAI-A, but we will not introduce them to the optimization. However, we will introduce constraints in order to limit MAI-R with respect to a design parameter $\mu \in \mathbb{R}^+$

$$\int_{-B}^{B} |H(f)|^2\, \Phi_R(f)\, df \leq \mu. \quad (13)$$

NONLINEAR MULTI-OBJECTIVE PROBLEM

We can establish a nonlinear multi-objective optimization problem with several constraints. We apply the weighting method [7]. The weighting method aggregates the multiple objectives linearly into a single objective function. Weights are applied to derive a weighted sum of the different objective functions. The first objective is to minimize the CRLB (5), thus to maximize $\int_{-B}^{B} f^2 |H(f)|^2\, df$ subject to $\int_{-B}^{B} |H(f)|^2\, df = 1$. The second objective is to maximize (8) and the third objective is to maximize (9). The first and second objective functions can be normalized with respect to B^2 and $\chi_0(\varrho)$ as shown in (7) and (8), respectively. The third objective function does not need to be normalized, as shown in (10). We also introduce a constraint to achieve a smooth cut-off following (11) and further constraints in order to limit MAI-R given in (13).

In order to transform the primal variational problem into a dual parametric optimization problem we use an adequate set of strictly band-limited orthonormal basis functions. Due to their special properties we propose to use the PSWF $\psi_m(\varrho, t)$ [5] and we define the expansion

$$h(t) = \sum_{m=0}^{M-1} x_m\, \psi_m(\varrho, t) \quad (14)$$

and

$$H(f) = \sum_{m=0}^{M-1} x_m\, \Psi_m(\varrho, f), \quad (15)$$

where $\Psi_m(\varrho, f)$ denotes the Fourier transform of $\psi_m(\varrho, t)$ and $x_m \in \mathbb{R}$ are the expansion coefficients. In particular, the PSWF have the very interesting property of being orthonormal in $]-\infty, \infty[$ and also being orthogonal in the finite interval $[-T_c/2, T_c/2]$.

Now, we can formulate the parametric nonlinear multi-objective optimization problem as a weighted sum of three quadratic forms with the weights w_1, w_2, and w_3:

$$\max_{\mathbf{x}} \left\{ \mathbf{x}^{\mathrm{T}} \left(\frac{w_1}{B^2}\, \mathbf{S}(\varrho) + \frac{w_2}{\chi_0(\varrho)}\, \mathbf{T}(\varrho) + w_3\, \mathbf{B}(\varrho) \right) \mathbf{x} \right\}, \quad (16)$$

$$\text{s.t. } ||\mathbf{x}||_2^2 = 1, \quad (17)$$

$$\mathbf{G}^{\mathrm{T}}\, \mathbf{x} = \mathbf{0}, \quad (18)$$

$$\forall_{i\in\{1,2,3\}}\ w_i \in [0, 1], \quad (19)$$

$$\text{and } \sum_{i=1}^{3} w_i = 1. \quad (20)$$

Here,

$$\mathbf{S}(\varrho) = \begin{bmatrix} s_{0\,0} & \cdots & s_{0\,N-1} \\ \vdots & \ddots & \vdots \\ s_{M-1\,0} & \cdots & s_{M-1\,N-1} \end{bmatrix} \in \mathbb{R}^{M\times M}, \quad (21)$$

where $s_{m\,n} = \int_{-\infty}^{\infty} f^2\, \Psi_m(\varrho, f)\, \Psi_n^*(\varrho, f) df$, $n = 0, \ldots, N-1$, and

$$\mathbf{T}(\varrho) = \text{diag}\{\boldsymbol{\chi}(\varrho)\} \in \mathbb{R}^{M\times M}, \quad (22)$$

where, $\boldsymbol{\chi}(\varrho) = [\chi_0(\varrho), \ldots, \chi_{M-1}(\varrho)]^{\mathrm{T}} \in \mathbb{R}^{M\times 1}$. Further,

$$b = \left[\int_{-B}^{B} H_b^*(f)\, H(f)\, df\right]^2 = \mathbf{x}^{\mathrm{T}}\, \mathbf{b}\mathbf{b}^{\mathrm{T}}\, \mathbf{x} = \mathbf{x}^{\mathrm{T}}\, \mathbf{B}(\varrho)\, \mathbf{x}, \quad (23)$$

with $\mathbf{b} = [b_0, \ldots, b_{M-1}]^{\mathrm{T}} \in \mathbb{R}^{M\times 1}$, $b_m = \int_{-B}^{B} H_b^*(f)\, \Psi_m(\varrho, f)\, df$, and $\mathbf{x} = [x_0, \ldots, x_{M-1}]^{\mathrm{T}} \in \mathbb{R}^{M\times 1}$ denotes the decision vector. The constraint matrix $\mathbf{G}$ is defined as

$$\mathbf{G} = [\mathbf{f}_R\ \mathbf{f}_I\ \mathbf{q}_1\ \ldots\ \mathbf{q}_d] \in \mathbb{R}^{M\times(2+d)}, \quad (24)$$

with

$$\mathbf{f}_R = [\text{Re}\{\Psi_0(\varrho, B)\}, \ldots, \text{Re}\{\Psi_{M-1}(\varrho, B)\}]^{\mathrm{T}} \in \mathbb{R}^{M\times 1}, \quad (25)$$

and

$$\mathbf{f}_I = [\text{Im}\{\Psi_0(\varrho, B)\}, \ldots, \text{Im}\{\Psi_{M-1}(\varrho, B)\}]^{\mathrm{T}} \in \mathbb{R}^{M\times 1}, \quad (26)$$

which achieve a smooth cut-off. $\mathbf{q}_1, \ldots, \mathbf{q}_d$ denote the $d \in \mathbb{N}$ dominant eigenvectors of $\mathbf{M}(\varrho)$, where

$$\int_{-B}^{B} |H(f)|^2 \, \Phi_R(f) \, df = \mathbf{x}^{\mathrm{T}} \, \mathbf{M}(\varrho) \, \mathbf{x} \leq \mu, \qquad (27)$$

with

$$\mathbf{M}(\varrho) = \begin{bmatrix} m_{0\,0} & \cdots & m_{0\,N-1} \\ \vdots & \ddots & \vdots \\ m_{M-1\,0} & \cdots & m_{M-1\,N-1} \end{bmatrix} \in \mathbb{R}^{M \times M}, \qquad (28)$$

where $m_{m\,n} = \int_{-B}^{B} \Psi_m(\varrho, f) \, \Psi_n^*(\varrho, f) \; \Phi_R(f) df$. MAI-R is limited by choosing d such that (27) is fulfilled with respect to a defined $\mu \in \mathbb{R}^+$.

The defined nonlinear multi-objective optimization problem results to an eigenvalue problem with respect to the trade-off introduced by the weights, as the matrices $\mathbf{S}(\varrho)$, $\mathbf{T}(\varrho)$, $\mathbf{B}(\varrho)$, and $\mathbf{M}(\varrho)$ are positive semi-definite. Thus, the complete Pareto optimal set can be easily generated.

PARETO OPTIMAL FINAL SOLUTIONS

We consider a design example in the E1/L1 band for GNSS with a time-bandwidth product $\varrho = 7$ where the chip duration is $T_c = 977.51$ ns and the bandwidth $B = 7.161$ MHz. Backward compatibility of the the new design is considered with respect to a BOC(1,1) signal in E1/L1 band, thus $|H_b(f)|^2$ is given by the PSD of a BOC(1,1) signal. We compare the selected designs to the Galileo E1-C pilot signal, CBOC(6,1,1/11,'-').

A maximum ΔSNR, ΔSNR_{max} using (12) is considered. We assume that $P_u = -154$ dBW for all u which is the maximum power defined for the Galileo Open Service [3], that $U = 11$ which is the maximum number of visible Galileo satellites which contribute to MAI-A, that $P_v = -158$ dBW for all v which is the nominal power defined for GPS M code signal [10], that $V = 12$ which is the maximum number of visible GPS satellites which contribute to MAI-R, that $\Phi_R(f)$ to be the PSD of GPS M-code signal , and that $N_0 = -204$ dBW/Hz. In order to assess the timing synchronization accuracy we define the CRLB-I as a lower bound which considers noise plus ICI, maximum MAI-A, and maximum MAI-R:

$$\tilde{\sigma}_\tau^2 \geq \sigma_\tau^2 \cdot \Delta\text{SNR}_{max}. \qquad (29)$$

In order to achieve a limited MAI-R we only introduce one dominant eigenvector ($d = 1$) of $\mathbf{M}(\varrho)$ to the constraint matrix $\mathbf{G}$. We will see in the following, that this yields acceptable levels of MAI-R for all the derived final solutions. With a more restrictive choice of the design parameter μ and thus larger d, further reduction of MAI-R could be achieved.

We consider the PSWF with $M = 40$, which provides sufficient precision for deriving the Parteo optimal set and the final solutions. Out of the Pareto optimal set we select the final solutions OPT1 and OPT2. In Table 1 κ, $\sqrt{b}$ with respect to a BOC(1,1) signal, ICI_{max}, MAI-A_{max}, MAI-R_{max}, and ΔSNR_{max} are shown for OPT1, OPT2, and Galileo E1-C pilot signal given that $B = 7.161$ MHz[1].

	OPT1	OPT2	E1-C
κ	0.54	0.6	0.58
$\sqrt{b}$	0.92	0.87	0.96
ICI_{max}	$2 \cdot 10^{-4}$	0.0022	$2 \cdot 10^{-5}$
MAI-A_{max}	0.23	0.20	0.31
MAI-R_{max}	0.003	0.004	0.02
ΔSNR_{max}	1.23 (0.90 dB)	1.21 (0.83 dB)	1.33 (1.24 dB)

Table 1 κ, $\sqrt{b}$, ICI_{max}, MAI-A_{max}, MAI-R_{max}, and ΔSNR_{max} with respect to $B = 7.161$ MHz.

In Figure 1 and Figure 2 the normalized spectrum $|H(f)|^2$ and the autocorrelation function $R_c(\varepsilon)$ are depicted for the final solutions OPT1 and OPT2. Also $\Phi_R(f)$ (GPS M code) and $R_c(\varepsilon)$ for the Galileo E1-C signal are given.

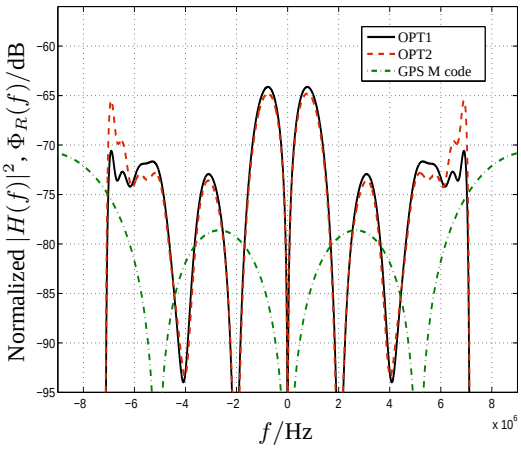

Fig. 1 Frequency domain.

In Figure 3 the CRLB-I is depicted for OPT1, OPT2, and the Galileo E1-C signal considering ΔSNR_{max} as given in Table 1.

[1]Nota bene: The presented design examples to show how the proposed method can be used in a practical case study of the E1/L1 band are not considered by Centre National d'Etudes Spatiales (CNES) and by German Aerospace Center (DLR) as sufficiently spectrally separated from the GPS M code.

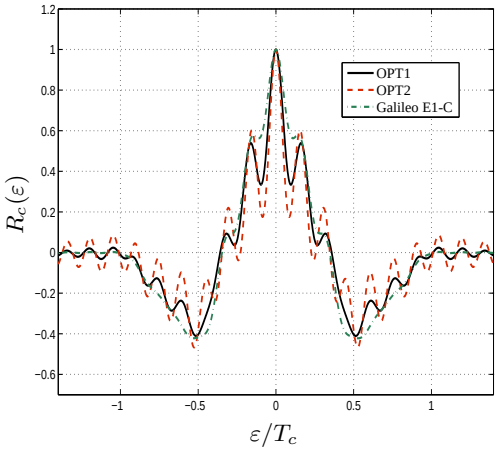

Fig. 2 Autocorrelation function.

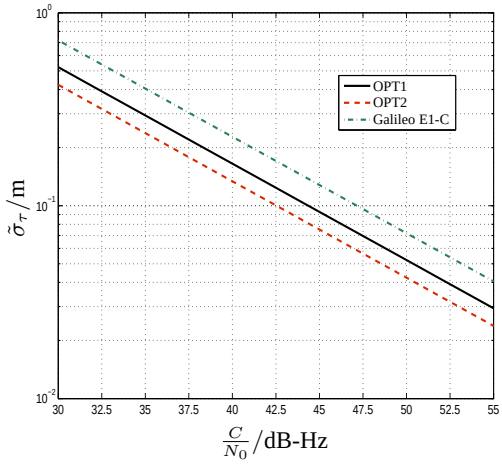

Fig. 3 CRLB-I.

PAYLOAD AND RECEIVER ANALYSIS

In this section an analysis of the performance of OPT1, OPT2, and the Galileo E1-C signal with respect to implementation on a payload and in a GNSS receiver is conducted following [11, 12]. In order to evaluate nonlinear behavior and potential spectral re-growth due to the high power amplifier (HPA) a solid state power amplifier (SSPA) is considered to evaluate the resulting correlation loss (CL) and power loss (PL). Furthermore, 8 bit quantization of the signal at the payload and 3 bit quantization at the receiver are assumed.

Fist we consider the case that OPT1, OPT2, and E1-C are transmitted by the payload and are also implemented for signal processing at the receiver with a receive bandwidth $B_r = B = 7.161$ MHz. Table 2 shows the CL and PL for the different signals for 0 dB output power back off (OPBO). OPT1 and OPT2 have a PL that is equal or close to 0 dB as they are strictly band-limited to $[-B, B]$ and no significant spectral re-growth is introduced by the SSPA.

	OPT1	OPT2	E1-C
CL	0.11 dB	0.13 dB	0.26 dB
PL	0 dB	0.01 dB	0.17 dB

Table 2 Power loss (PL) and correlation loss (CL).

In Figure 4 the root-mean square (RMS) time-delay tracking error of a non-coherent delay locked loop (DLL) with coherent integration time $T_p = 100$ ms, early-late correlator spacing $\Delta = 0.06\,T_c$, and $B_n = 1$ Hz is depicted for OPT1, OPT2, and for E1-C signal. In Figure 4 only the degradation of the performance by signal quantization at receiver and payload level are included. PL, CL, and ΔSNR_{max} are not included in Figure 4.

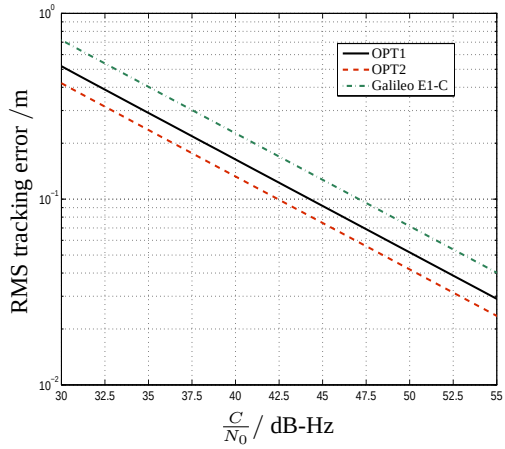

Fig. 4 RMS time-delay tracking error, $T_p = 100$ ms, $B_n = 1$ Hz, $\Delta = 0.06\,T_c$.

In Figure 5 the multipath error envelope for OPT1, OPT2, and E1-C signal is shown.

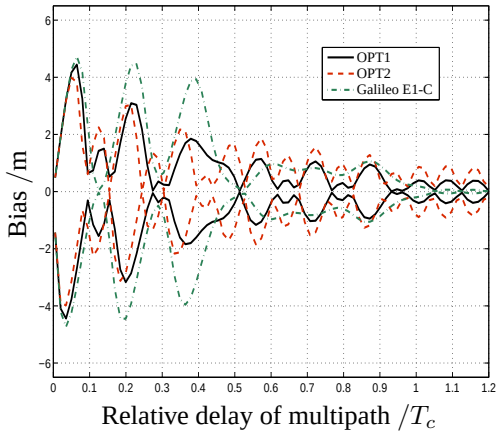

Fig. 5 Multipath error envelope.

Secondly, we consider the case that OPT1, OPT2, and E1-C are transmitted by the payload and a BOC(1,1) signal is implemented for signal processing at the receiver with a receive bandwidth $B_r = 4.092$ MHz. Table 3 shows the CL and PL for the different signals for 0 dB OPBO.

	OPT1	OPT2	E1-C
CL	0.36 dB	0.36 dB	0.35 dB
PL	1.28 dB	1.94 dB	0.76 dB

Table 3 Power loss (PL) and correlation loss (CL) considering BOC(1,1) processing with $B_r = 4.092$ MHz.

In Figure 6 the RMS time-delay tracking error of a non-coherent DLL with a coherent integration time $T_p = 100$ ms, a early-late correlator spacing $\Delta = 0.1\,T_c$, and $B_n = 1$ Hz is depicted for OPT1, OPT2, and E1-C signal implementing a BOC(1,1) signal for signal processing at the receiver. In Figure 6 of the performance by signal quantization at receiver and payload level are included. PL, CL, and ΔSNR_{max} are not included in Figure 6. We can observe, that backward compatibility is achieved taking into account implementation aspects at payload and receiver level.

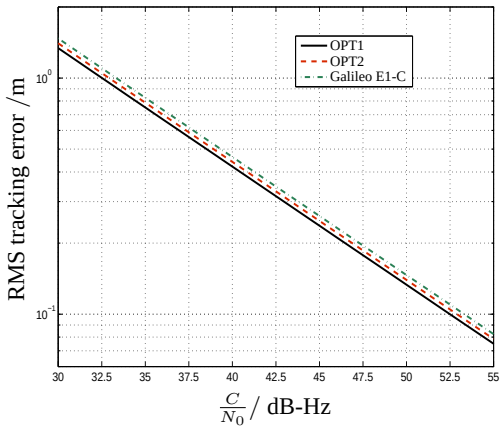

Fig. 6 RMS time-delay tracking error considering BOC(1,1) at the receiver with $B_r = 4.092$ MHz, $T_p = 100$ ms, $B_n = 1$ Hz, and $\Delta = 0.1T_c$.

CONCLUSION

The proposed methodology for optimum chip pulse shape design provides a flexible and systematic approach in order to account for all important properties for timing synchronization, especially for GNSS. The complete Pareto optimal set of the defined nonlinear multi-objective problem can be easily derived by solving the resulting weighted sum of three quadratic forms in terms of an eigenvalue problem. Thus, chip pulse shapes which are optimized for timing synchronization performance and which additionally consider backward compatibility with respect to current signals can be derived. These optimized chip pulse shapes provide significant service improvement for timing synchronization, even taking into account implementation aspects at payload and receiver level.

REFERENCES

[1] M. A. Landolsi and W. E. Stark, "DS-CDMA Chip Waveform Design for Minimal Interference Under Bandwidth,Phase, and Envelope Constraints," *IEEE Transactions on Communications*, vol. 47, no. 11, 1999.

[2] M. A. Landolsi, "Perfromance Limits in DS-CDMA Timing Acquisition," *IEEE Transactions on Wireless Communications*, vol. 6, no. 9, 2007.

[3] J. V. P. Gisbert, "Interference Assessment Using up to Date Public Information of Operating and under Development RNSS Systems," in *Fourth European Workshop GNSS Signals 2009*, Oberpfaffenhofen, Germany, Dezember 2009.

[4] F. Antreich and J. A. Nossek, "Optimum Chip Pulse Shape Design for Timing Synchronization," in *Proceedings of the 36th IEEE International Conference on Acoustics, Speech and Signal Processing ICASSP*, Prague, Czech Republic, Mai 2011.

[5] D. Slepian and H. O. Pollak, "Prolate Spheroidal Wave Functions, Fourier Analysis and Uncertainty - I," *Bell System Technical Journal*, vol. 40, no. 1, 1961.

[6] F. Antreich, J. A. Nossek, J.-L. Issler, and M. Meurer, "On Methodologies for GNSS Signal Design," in *Proceedings of 4th European Workshop on GNSS Signals and Signal Processing*, Oberpfaffenhofen, Germany, Dezember 2009.

[7] K. M. Miettinen, *Nonlinear Multiobjective Optimization*. Kluwer Academic Publishers, U.S.A., 1999.

[8] S. M. Kay, *Fundamentals of Statistical Signal Processing: Estimation Theory*. Prentice Hall PTR, 1993, vol. 1.

[9] A. J. Viterbi, *CDMA: Principles of Spread Spectrum Communication*. Addison-Wesley Publishing Company, 1995.

[10] W. Marquis and M. Shaw, "GPS III, Bringing New Capabilities to the Global Community," *InsideGNSS*, September/October 2011.

[11] J.-J. Floch, F. Antreich, J.-J. Issler, and M. Meurer, "Comparison of Different Chip Pulse Shapes for DS-CDMA Systems," in *Proceedings of IEEE/ION PLANS 2010*, Palms Springs, CA, U.S.A., Mai 2010.

[12] J.-J. Floch, F. Antreich, M. Meurer, and J.-J. Issler, "S-Band Signal Design Considering Interoperability and Spectral Separation," in *Proceedings of 23th Annual International Technical Meeting ION GNSS 2010*, U.S.A., Portland, Oregon, September 2010.